Description of Modal Gating of the Cardiac Calcium Release Channel in Planar Lipid Membranes

Alexandra Zahradníková and Ivan Zahradník
Institute of Molecular Physiology and Genetics, Slovak Academy of Sciences, 833 34 Bratislava, Slovak Republic

ABSTRACT Single channel activity of the cardiac ryanodine-sensitive calcium-release channel in planar lipid membranes was studied in order to elucidate the calcium-dependent mechanism of its steady-state behavior. The single channel kinetics, observed with Cs^+ as the charge carrier at different activating (*cis*) Ca^{2+} concentrations in the absence of ATP and Mg^{2+}, were similar to earlier reports and were extended by analysis of channel modal behavior. The channel displayed three episodic levels of open probability defining three gating modes: H (high activity), L (low activity), and I (no activity). The large difference in open probabilities between the two active modes resulted from different bursting patterns and different proportions of two distinct channel open states. I-mode was without openings and can be regarded as the inactivated mode of the channel; L-mode was composed of short and sparse openings; and H-mode openings were longer and grouped into bursts. Modal gating may explain calcium-release channel adaptation (as transient prevalence of H-mode after Ca^{2+} binding) and the inhibitory effects of drugs (as stabilization of mode I), and it provides a basis for understanding the regulation of calcium release.

INTRODUCTION

Excitation-contraction coupling in the heart involves calcium-induced calcium release (Fabiato, 1985; Cannell et al., 1987; Näbauer et al., 1989; Sipido and Wier, 1991; Cleeman and Morad, 1991). Influx of calcium ions via the plasma membrane triggers much larger release of calcium ions from the terminal cisternae of the sarcoplasmic reticulum through the ryanodine-sensitive calcium-release channels (CRCs). The mechanisms by which this calcium release is terminated are not fully understood. Using the skinned cardiac muscle preparation, Fabiato (1985) reported direct inactivation of calcium release by cytoplasmic calcium. However, Ca^{2+}-dependent inactivation of single CRCs was not confirmed in planar lipid bilayer experiments. Native and purified sarcoplasmic reticulum (SR) CRCs have both maintained activity even at *cis* (cytoplasmic) Ca^{2+} concentrations as high as 1 mM (Rousseau and Meissner, 1989; Ashley and Williams, 1990; Chu et al., 1993). The observed calcium dependence of open probability was S-shaped (saturating above 100 μM Ca), in contrast to skeletal muscle CRC or inositol trisphosphate receptors (Smith et al., 1988; Chu et al., 1993; Bezprozvanny et al., 1991), in which a bell-shaped dependence (decrease of P_o above 100 μM Ca) was measured, as expected for the inactivation of the channel at high Ca^{2+} concentrations.

Györke and Fill (1993) measured the response of the ryanodine receptor/CRC to a rapid increase of *cis*-Ca^{2+}. They detected transients of single channel activity that showed bursts of closely spaced openings immediately after activation and decayed later into more isolated openings. Channel activity at the peak of the response was found more sensitive to calcium than activity after relaxation to steady state. However, no dependence of inactivation rate on *cis* Ca^{2+} concentration was found. These characteristics of the CRC were termed "adaptation" (Györke and Fill, 1993). It is not clear whether these functions are intrinsic properties of the channel or whether they are mediated by a regulatory molecule. In either case, additional insight into channel gating mechanisms is required in order to understand how adaptation occurs. To this end, Zahradníková and Zahradník (1993) used the gating scheme of Zahradníková and Palade (1993) to simulate adaptation. This model, which includes a long-lived closed state, can simulate transient responses of the channel to calcium steps. However, the modeled responses were smaller and showed much slower activation than those measured experimentally (Györke and Fill, 1993; Györke et al., 1994). To develop models of CRC gating further, we needed more detailed experimental data.

Here we present results of single channel measurements of the cardiac CRC with 200 μs temporal resolution at several concentrations of activating Ca^{2+}. The results of our analysis of closed times could not explain the behavior of the channel over a time scale of seconds. Rather, the channel seemed to episodically cycle between periods with no activity, periods with intermediate levels of activity, or periods with high levels of activity. Periods of intermediate and high activity differed in the relative contribution of multiple open and closed lifetimes to the kinetics of the channel. Such complex behavior can be explained with a complex kinetic scheme incorporating many states, interconnected by fast or slow gating steps. To simplify such models, and to make them tractable for detailed analysis, the episodic kinetic alterations can also be considered "mode" shifts (Patlak et al., 1979; Hess et al., 1984; Blatz and Magleby, 1986). In modes, a subset of states describes

Received for publication 6 January 1995 and in final form 8 August 1995.
Address reprint requests to Dr. Alexandra Zahradníková, Institute of Molecular Physiology and Genetics, Slovak Academy of Sciences, Vlárska 5, 83334 Bratislava, Slovakia. Tel.: 42-7-375-266; Fax: 42-7-373-666; E-mail: umfgzahr@savba.sk.

0006-3495/95/11/1780/00 $2.00

channel activity, and transitions between individual modes do not necessarily imply a specific pathway between channel states. That modes are a sensible simplification of complex gating and might represent physiologically relevant subsets of channel conformations is supported by the existence of effectors that act via effect on probability of modes (Patlak and Ortiz, 1985; Fox et al., 1986; Imredy and Yue, 1994). We report here stochastic analysis of CRC activity with respect to its modal gating. This approach revealed at least three modes of channel activity that have properties compatible with transient responses to step channel activation.

MATERIALS AND METHODS

Bilayer experiments

Canine cardiac microsomal fraction was prepared by the procedure of Harigaya and Schwartz (1969), modified as described in Zahradníková and Palade (1993). In brief, hearts were removed under pentobarbital anesthesia. Left ventricles, cleaned of connective tissue and vessels, were minced and then homogenized with a Polytron homogenizer in 3 vol of 0.9% NaCl buffered with 10 mM Tris(hydroxymethyl)-aminomethane (pH 7.3). The homogenate was centrifuged at 4000 × *g* for 20 min, then recentrifuged at 8000 × *g* (20 min) and 40,000 × *g* (30 min) to obtain two crude microsomal fractions that were resuspended in the above saline plus 10% sucrose, frozen, and stored in liquid nitrogen. CsOH (Aldrich, Milwaukee, WI) and methane sulfonic acid (Fluka, Buchs, Switzerland) were used for preparation of $CsCH_3SO_3$. Other chemicals (except when specifically noted) were from Sigma (St. Louis, MO).

Synthetic lipids (Avanti Polar Lipids, Birmingham, AL, or Sigma) were used to prepare bilayers of the composition 5:3:2 phosphatidyl serine/phosphatidyl ethanolamine/phosphatidyl choline (50 mg/ml in decane, Aldrich, Milwaukee, WI). A Teflon partition with a 0.15-mm aperture was used. Solutions of 250 mM (*cis*, the SR application side, corresponding to the cytoplasmic side) and 50 mM $CsCH_3SO_3$ (*trans*) buffered with 5 mM CsMOPS to pH 7.4, containing 5 μM Ca^{2+}, were used to isolate CRC activity from that of other channel types (Chu et al., 1993; Zahradníková and Palade, 1993). The desired *cis* Ca^{2+} concentration was obtained by adding calcium methane sulfonate or Cs_2EGTA (in an amount calculated according to Fabiato, 1988) and was verified with a calcium selective electrode (Radiometer, Copenhagen, Denmark). The CRC was identified on the basis of its conductance (440 ± 10 pS) and its responsiveness to agonists (100 μM calcium, 1 mM ATP, 10 μM ryanodine (Calbiochem, Lucerne, Switzerland)) as well as to inhibitors (e.g., 2 μM ruthenium red (Aldrich, Milwaukee, WI), 3 mM $MgCl_2$).

Data acquisition and analysis

Single-channel currents were measured with a bilayer amplifier designed according to Hamilton et al. (1989). A 286 AT computer with pCLAMP software (Axon Instruments, Foster City, CA) was used for data collection. Data were filtered at 2 kHz with an 8-pole Bessel filter, stored on VHS tape using a PCM recorder (Vetter model 200, Rebersburg, PA), and digitized at 5 kHz off-line with a Labmaster (Scientific Solutions, Solon, OH) interface. Stretches of single-channel activity of at least 1-min duration were analyzed using an AT 486 computer with pCLAMP, IPROC, and TRANSIT software (Axon Instruments; Baylor College of Medicine, Houston, TX). The shortest event duration included in the analysis was 200 μs, which was more than twice the filter dead time (90 μs). The noncumulative histograms of open and closed times, fitted by sums of exponentials using the minimum χ^2 method, as well as all other secondary analyses, calculations, and statistics, were carried out using Origin (Microcal Software, Northampton, MA). Statistical significance was evaluated by Student's *t*-test. The results are presented as mean ± SEM. Contingency tables were analyzed using InStat (GraphPAD Software, San Diego, CA). Symbolic integration was performed in Mathematica (Wolfram Research, Champaign, IL).

Bursts of openings were categorized for analysis using a value of the critical closed time, t_c, giving equal numbers of misclassified short and long closures (Magleby and Pallotta, 1983). The value of t_c was calculated for every channel according to the formula below, where W_{ci} and τ_{ci} stay for the areas and time constants, respectively, of the i-th closed state:

$$W_{c1}\exp\left(-\frac{t_c}{\tau_{c1}}\right) + W_{c2}\exp\left(-\frac{t_c}{\tau_{c2}}\right) = W_{c3}\left(1 - \exp\left(-\frac{t_c}{\tau_{c3}}\right)\right).$$

Numbers of openings per burst were fitted by the geometric distribution (Colquhoun and Sigworth, 1983):

$$P(r) = \sum_i W_{ni}(1/n_{bi})(1 - 1/n_{bi})^{r-1},$$

where $P(r)$ is the probability of observing a burst with r openings and W_{bi} and n_{bi} are the relative areas and mean numbers of openings per burst, respectively, of the distributions.

For the interpretation of modal behavior, it is important that events observed over a long period arise from the same single channel. Therefore, care was taken to assure that no multiple channels were present. The 12 channels included in analysis were selected as satisfying single-channel criteria from a set of ~150 bilayer measurements.

RESULTS

Calcium dependence of channel gating

Examples of channel activity at four different Ca^{2+} concentrations, spanning the range from very low to full activation, are shown in Fig. 1. The estimated values of open and closed lifetimes were not significantly dependent on Ca^{2+} in these experiments (Table 1). The increase in open probability with increasing calcium concentration seems to result solely from a profound change in the relative areas of the three closed time components with Ca^{2+}. This was manifested in the general appearance of the records (Fig. 1), which consisted of three activity patterns: spike-like openings appearing at random, closely spaced bursts of openings, and long silent periods. In low Ca^{2+} concentrations,

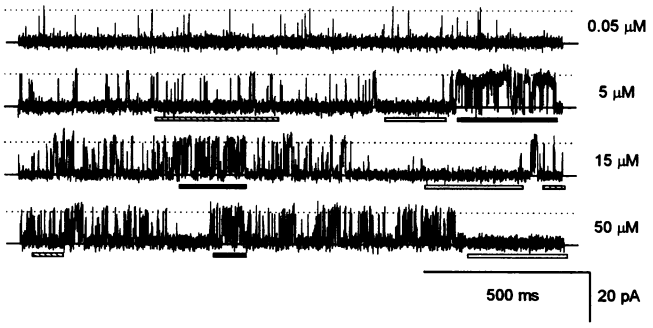

FIGURE 1 Activity of the cardiac calcium release channel at different activating *cis* Ca^{2+} concentrations. Typical traces of the steady-state CRC activity in planar lipid bilayers after activation by different Ca^{2+} concentrations (*right*). Full line denotes closed level; dotted line represents open level of the channel. The three types of activity (high open probability, low open probability, and long closures) are denoted by black, hatched, and white bars below the traces.

TABLE 1 Cardiac calcium-release channel lifetime parameters at different Ca^{2+} concentrations

		Calcium concentration [μM]			
	i	0.05 (n = 3)	5 (n = 7)	15 (n = 5)	50 (n = 2)
Open time τ_{oi} (ms)	1	0.29 ± 0.07	0.37 ± 0.03	0.32 ± 0.02	0.34 ± 0.02
	2	4.23 ± 1.63	2.90 ± 0.27	2.41 ± 0.38	3.00 ± 0.78
Relative area W_{oi}	1	0.88 ± 0.08	0.77 ± 0.05	0.83 ± 0.03	0.89 ± 0.04
	2	0.12 ± 0.08	0.23 ± 0.05	0.17 ± 0.03	0.11 ± 0.04
Closed time τ_{ci} (ms)	1	0.56 ± 0.17	0.37 ± 0.04	0.32 ± 0.05	0.38 ± 0.15
	2	6.70 ± 1.24	4.34 ± 0.53	5.15 ± 0.34	2.54 ± 0.15
	3	167.5 ± 46.6	166.4 ± 81.3	48.3 ± 5.9	92.4 ± 52.3
Relative area W_{ci}	1	0.02 ± 0.01	0.11 ± 0.03	0.17 ± 0.03	0.27 ± 0.02
	2	0.05 ± 0.04	0.13 ± 0.03	0.37 ± 0.07	0.53 ± 0.07
	3	0.94 ± 0.04	0.75 ± 0.06	0.46 ± 0.07	0.19 ± 0.05
Open probability		0.001 ± 0.0001	0.06 ± 0.02	0.04 ± 0.01	0.11 ± 0.02

only spiking activity was observed, whereas all three activity patterns were present at intermediate and high calcium concentrations. Long closures were still prominent at higher Ca^{2+}. The relative area of the long closed time decreased, whereas those of the short and medium closed time increased with increasing *cis* Ca^{2+}. The open probability (P_o, Table 1) therefore increased in response to elevated *cis* Ca^{2+}. As neither of the open lifetimes is Ca^{2+}-dependent, missed events shorter than 200 μs should not influence these trends. On the other hand, absolute values of the time constants are influenced by the 2-kHz filtering.

Analysis of slow changes in channel gating

None of the gating transitions described above can account for slow alterations of P_o on a time scale of seconds, which we observed. Although not directly discernible from the closed time distributions, these alterations are manifested in the large standard errors of τ_{c3} (Table 1; note smaller errors of τ_{c3} in Table 4). Zahradníková and Palade (1993) tentatively attributed the same slow process to transitions between modes. Signs of modal behavior of the CRC can be also discerned in records of CRC activity published by others.

Fig. 2 demonstrates an analysis of modes using the method of Hess et al. (1984) for a typical channel measured at 15 μM Ca^{2+}. Segment length was set to 409.6 ms, the minimal length allowed by the software, which was found to be acceptable. Open probability, P_o, was determined for each segment as the total open time of the segment divided by its duration (409.6 ms). A plot of P_o against time (Fig. 2 *B*, *top*) indicates that segments with no openings, segments of low P_o, and segments of high P_o appear in clusters. Analysis of clustering of segments can be used to determine whether CRC gating is nonuniform, or "modal". For this analysis individual segments needed to be classified by their putative mode. The classification criterion for distinguishing between modes L and H was found from the plot of frequency distribution of P_o (Fig. 2 *C*), where the minimum can be used as a threshold open probability, P_m, separating apparent modes. The low P_o segments ($0 < P_o \leq 0.10$) occurred 325 times, and the high P_o segments ($P_o > 0.10$) were identified 167 times. Segments with $P_o = 0.0$ were observed 18 times.

When such classifications were plotted as they occurred in the record, we obtained a picture (Fig. 2 *B*, *bottom*) strongly suggestive of episodic changes. The presence of modes, i.e., clustering of segments in a way that deviates from statistical independence (Fisher, 1958), can be tested by application of the χ^2 test to a contingency table containing the observed frequencies of two successive segments of a specific type (Nowycky et al., 1985). This analysis was performed for 12 channels measured at intermediate Ca^{2+} concentrations (7 channels at 5 μM Ca^{2+}, 5 channels at 15 μM Ca^{2+}) for longer than 100 s each. The average threshold open probability, P_m, was 0.1 ± 0.01. Average values for P_o in low-activity and high-activity segments were 0.021 ± 0.004 and 0.20 ± 0.04, respectively. In every channel the sequence of segments was found to deviate strongly from that expected for a random distribution ($\alpha < 0.0005$ for 11 channels and $\alpha < 0.01$ for 1 channel with high prevalence of mode L). Moreover, we have observed a systematic pattern in contingency tables in which the diagonal cells showed higher than random frequencies, and nondiagonal cells showed frequencies lower than random. To determine whether all 12 experiments have the same pattern, we constructed, in analogy to a contingency table, a table of average probabilities (±SEM) of any combination of segment pairs occurring in succession (Table 2, upper lines) together with the probabilities of random occurrence of these sequences (Table 2, lower lines). It can be seen that the probability of observing nonidentical mode segments in sequence is four times lower than if they had occurred at random. In contrast, the probability of observing a given segment type twice in succession is about three times higher than random occurrence predicts. This analysis confirms that consecutive segments hold a similar pattern of gating, consistent with episodic or modal behavior. Table 2 also indicates that transitions between modes are not random. The probability of finding modes I and H after each other is

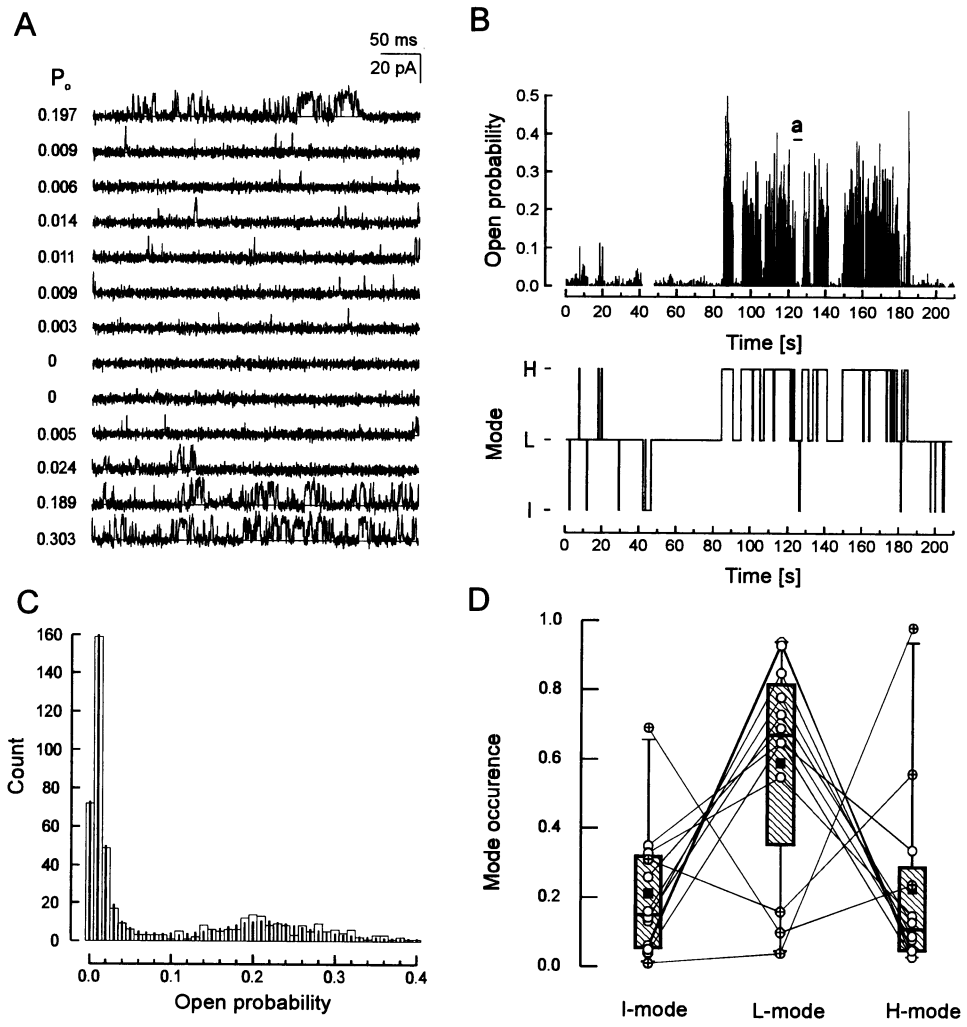

FIGURE 2 Modal characteristics of the calcium release channel. Modal behavior is illustrated here on a 220-s long, typical continuous record of the channel activated by 15 μM Ca^{2+}. (*A*) Selected 13 contiguous segments of the record (corresponding to the region *a* in part *B*) showing three different types of activity: high-P_o segments (lines 1, 12, 13), low-P_o segments (2–7, 10, 11), and null segments (8, 9). Segment duration is 409.6 ms. Open probability (P_o) during the respective segments is indicated at the left. (*B*) Top shows channel open probability in segments shown as a function of time. Horizontal line (*a*) indicates the portion of the record shown in part A. Bottom shows modal representation of channel activity. Segments were classified as modes I, L, and H by their P_o value (see part *C*). (*C*) Frequency histogram of channel open probability from this experiment. The 18 segments without openings were not included in the analysis. The data (columns) were well fit by a double Lorentz curve $y = \sum_i \{2A_i w_i/[w_i^2 + 4(x - x_{ci})^2]\}$ (*vertical bars*) with parameters $A_1 = 1.94 \pm 0.02$, $x_{c1} = 0.02 \pm 0.0001$, $w_1 = 0.01 \pm 0.0002$, $A_2 = 1.11 \pm 0.12$, $x_{c2} = 0.21 \pm 0.006$, $w_2 = 0.13 \pm 0.02$. The curve has a minimum around $P_o = 0.1$, which defines the threshold open probability value (P_m) for distinguishing between modes L and H in this experiment. (*D*) Relative occurrence of modes I, L, and H in the analyzed population of 12 channels recorded at intermediate calcium concentration. The box plot shows population median and 5, 25, 75, and 95 percentiles. Filled squares represent the population mean. The values for individual channels are shown as circles connected by lines. Crossed circles represent a group of three channels dissimilar by low occurrence of L-mode.

much less than that of finding modes I and L or H and L together. This feature is analyzed in detail below.

All three modes of activity were detected in 11 of 12 channels, whereas 1 channel did not show the presence of mode I (that is, no 409.6 ms segment without an opening was found). The probability of occurrence of individual modes, calculated as ratio of the total time spent in the segments of the given type to the total length of analyzed record, is shown as box plots in Fig. 2 *D*. Interestingly, the relative occurrence of modes for individual channels is strongly scattered, which might imply heterogeneity in the measured population of channels. However, this variation may also be a consequence of modal gating, as the contribution of individual modes along records varied substantially. Variation in occurrence of active modes L and H was negatively correlated with the length of records, with correlation coefficients of -0.31 and -0.27, respectively. In steady state, the CRCs activated by $\sim$10 μM Ca^{2+} spent most of the time in L-mode; the relative occurrence of either mode H or mode I was almost three times smaller (see Table 3). Because of a much higher open probability in H-mode than in L-mode, the relative contributions of the two active modes to overall open probability were about the same (Table 3).

TABLE 2 Sequence probability table for the three modes of calcium-release channel gating

		Segment k		
		I-mode	L-mode	H-mode
Segment $k+1$	I-mode	**0.15 ± 0.05*** (0.04)	**0.05 ± 0.01‡** (0.12)	**0.006 ± 0.004‡** (0.04)
	L-mode	**0.05 ± 0.01‡** (0.12)	**0.50 ± 0.09*** (0.33)	**0.03 ± 0.01‡** (0.12)
	H-mode	**0.006 ± 0.004‡** (0.04)	**0.03 ± 0.01‡** (0.12)	**0.18 ± 0.08§** (0.05)

The probabilities of observed specified sequences of segments appearing in succession are given in boldface above the random predictions (in parentheses).
*Significantly more than random prediction at $p < 0.05$.
‡Significantly less than random prediction at $p < 10^{-6}$.
§Significantly more than random prediction at $p = 0.066$.

Intramodal behavior

In addition to their open probabilities, the two active modes (L and H) differ in duration and frequency of openings as well. This is convincingly illustrated in Figs. 2 *C* and 3 *A* and Table 3. Average open time determined in the illustrated experiment separately for each mode gave $t_o = 0.83 \pm 0.05$ ms and $t_o = 2.05 \pm 0.14$ ms for mode L and H, respectively. Combined data for all 12 experiments, as given in Table 3, show that in H-mode an average detected opening is about 2.3 times longer than in L-mode. Comparison of open time distributions for the mode L and H segments analyzed separately (Table 3) shows that the differences between the two segment types are due to different relative contributions of the same two open time components in the open time distributions (Table 1) and are not due to the presence of another open state.

The higher open probability within H-mode is also related to a higher number of openings per segment. On average, n_{o2} was 5 times higher than n_{o1} (see Table 3). Thus the relative contribution of closed times also participated in mode differences. To further characterize channel gating within the two active modes, we performed burst analysis for L-mode and H-mode segments separately (Table 4). The distribution of numbers of openings per burst was composed of two components, as was that of burst duration. Their relative contribution differed markedly for L-mode and H-mode segments. Single open events, giving rise to the short component of burst distribution, dominated in L-mode and were scarce in H-mode segments, whereas bursts with multiple openings forming long bursts dominated in H-mode segments. The duration of the shorter bursts (with τ_{b1} between 0.34 and 0.40 ms), close to the shorter open lifetime, suggests that single open events originate from the shorter open time component.

TABLE 3 Properties of the calcium-release channels in different modes of activity

		I-mode	L-mode	H-mode
Relative occurrence		0.20 ± 0.06	0.56 ± 0.09	0.22 ± 0.08
Average open time, t_o (ms)			1.04 ± 0.08	2.34 ± 0.32
Average number of openings per segment, n_o			8.36 ± 1.67	42.2 ± 5.8
Open probability, p_o		0.0	0.021 ± 0.004	0.20 ± 0.04
Relative contribution to overall open probability		0.0	0.44 ± 0.10	0.56 ± 0.10
Open state lifetimes τ_{oi} (ms)	1		0.38 ± 0.03	0.41 ± 0.06
	2		2.86 ± 0.26	2.77 ± 0.39
Relative areas, W_{oi}	1		0.90 ± 0.02	0.56 ± 0.04
	2		0.10 ± 0.02	0.44 ± 0.04

Missed events cannot account for modal differences

The distribution of open times in L-mode and H-mode (Table 3) predicts that in L-mode ~47% and in H-mode ~25% of all openings are missed at 0.2 ms time resolution. The average open time, corrected for missed events (calculated as weighted average from open lifetime parameters of Table 3), was 0.63 and 1.45 ms for L-mode and H-mode, respectively. As the proportions of the two open time components in the two modes are strikingly different and the ratio of average open time values before and after correction for missed events is almost the same, the main effect of events shorter than 0.2 ms on intramodal analysis will be a proportional increase in the average number of openings per segment. The increase in open probability will be negligible.

I-mode might, however, be an artifact from missing several short L-mode events in succession. Consider the following: the probability of a 409.6 ms stretch of missed openings, i.e., a "ghost" null segment, p(ghost), can be estimated as

$$p(\text{ghost}) = \sum_{i=0}^{\infty} p(i \text{ openings}) \cdot (p(\text{missed}))^i,$$

where $p(i$ openings) is the probability of occurrence of exactly i openings per segment, p(missed) is the probability of missing an opening, and i is the number of openings. An upper estimate for $p(i$ openings) can be obtained by disregarding the two faster closed lifetimes, calculating the probability density for the length of $(i+1)$ long closures along the lines described by Colquhoun and Hawkes (1983), and integrating the result from 409.6 ms to infinity. The probability of missing an opening in L-mode is 0.47 (see above). The calculation gives probability p(ghost) = 0.044 (compare with the I-mode occurrence of 0.20 ± 0.06), and the probability of observing two consecutive ghost null segments is $(0.044)^2 = 0.0019$. As we have identified 121 single, 71 double, and 77 multiple fully closed segments in our experiments, it is unlikely that I-mode could be caused by missed events.

Intermodal behavior

In Fig. 3 *A*, changes in segment characteristics are depicted for the same experiment that is shown in Fig. 2. The average

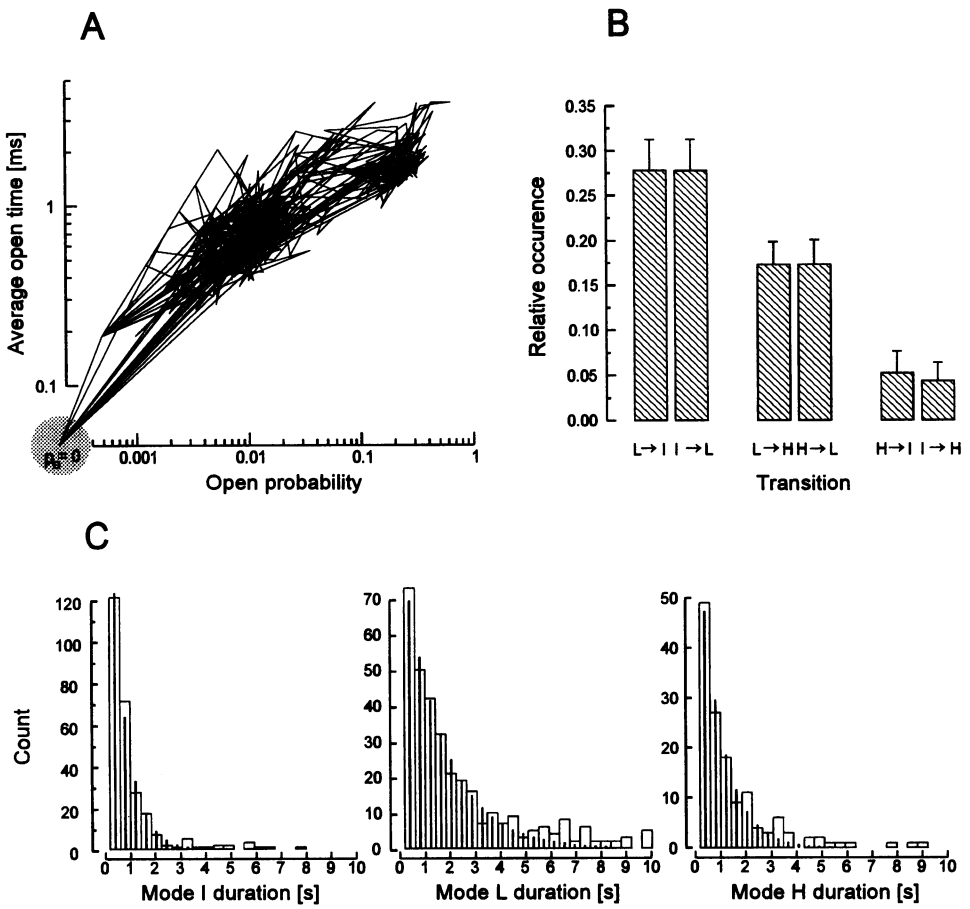

FIGURE 3 Intermodal transitions of the CRC. (*A*) Nested representation of modes. Average open time (mean duration of a single opening) within the segment is plotted against the P_o in the segment. Consecutive points are connected by straight lines. Null segments are shown as one point outside plot margins to better illustrate transitions between modes. Three nests visible in the plot represent modes I, L, and H (left to right). (*B*) Relative frequency of transitions between pairs of modes (the number of transitions of the given type divided by total number of transitions; mean ± SEM). Mean number of forward and backward transitions is statistically the same. (*C*) Histograms of mode durations, combined for all 12 channels, at intermediate calcium (2000 s of recording). Experimental data are shown as open boxes (bin width is set to segment duration of 409.6 ms). The monoexponential fits (*vertical bars*) provided values of τ_{MI} = 0.61 s, τ_{ML} = 1.60 s, and τ_{MH} = 0.86 s for the modes I, L, and H, respectively.

open time within each segment is plotted against P_o of that segment. The points from consecutive segments are connected by lines. The clustering of lines into regions of similar properties builds up nest-like patches and also reveals pathways of the transitions. This representation, which we call a nest-diagram, provides a simple and figurative means to assess both the presence of the modes and their transitions. The occurrence of lines between the nests, representing transitions between different modes, is much less than the density of lines within the nests, representing intramodal transitions. In the illustrated case, the transitions between the two nests of open states and between the closed and low-P_o nest were frequent, whereas no transitions to the closed nest came from the high-P_o nest. Because this observation may be important for the interpretation of modal gating, we tested its statistical significance.

TABLE 4 Closed lifetimes and burst distributions inside L-mode and H-mode segments

Parameter		*i*	L-mode	H-mode
Closed times	τ_{ci} (ms)	1	0.39 ± 0.03	0.38 ± 0.03
		2	4.10 ± 0.46	3.27 ± 0.34
		3	57.8 ± 8.4	59.1 ± 3.9
	W_{ci}	1	0.10 ± 0.01	0.34 ± 0.04
		2	0.12 ± 0.03	0.48 ± 0.04
		3	0.78 ± 0.03	0.18 ± 0.05
Critical closed time	t_c (ms)		3.69 ± 0.50	9.04 ± 0.75
Number of openings per burst	n_{bi}	1	1.19 ± 0.03	1.23 ± 0.05
		2	9.35 ± 5.54	4.89 ± 0.86
	W_{ni}	1	0.91 ± 0.03	0.16 ± 0.05
		2	0.09 ± 0.03	0.84 ± 0.05
Burst length	τ_{bi} (ms)	1	0.34 ± 0.02	0.40 ± 0.04
		2	16.3 ± 8.1	68.6 ± 23.8
	W_{bi}	1	0.76 ± 0.05	0.30 ± 0.05
		2	0.24 ± 0.05	0.70 ± 0.05

Fig. 3 *B* shows that the channel prefers certain transitions between modes (see also Table 2). Transitions from mode L to I and back (56% of transitions) were most frequent, and transitions between modes L and H (35% of transitions) were intermediate; shifts from H to I and back (9%) were rare. It is possible that transitions detected as I ↔ H are in fact two-step transitions with a sojourn in L-mode within a single segment. Average probabilities of I → L → H and H → L → I double transitions occurring within the same 409.6 ms segment was estimated to be 0.017 ± 0.003 and 0.029 ± 0.008, respectively. These values are not significantly different from the experimentally measured probabilities of I → H and H → I transitions, which were 0.028 ± 0.016 (n = 24) and 0.051 ± 0.017 (n = 28), respectively, on average from the 12 files (total of 786 transitions between modes).

The durations of channel sojourns in a particular mode can serve as an estimate of mode lifetime (inversely proportional to the rate of exit from the mode). Because there were too few transitions between modes in any single recording, we constructed histograms of mode durations from all 12 channels combined. These data are shown in Fig. 3 *C* together with the respective monoexponential fits, which yielded time constants, i.e., mode lifetimes, of $\tau_{MI} = 0.61$ s, $\tau_{ML} = 1.60$ s, and $\tau_{MH} = 0.86$ s.

DISCUSSION

Open and closed times

Previous reports indicated the presence of two (Ashley and Williams, 1990) or three (Chu et al., 1993; Sitsapesan and Williams, 1994) open time components in CRCs that are activated by Ca^{2+} alone. Our data confirmed the presence of the two shorter lifetime components. Inclusion of a third component did not improve χ^2 values significantly, even in segments with very different average open times, when analyzed separately. The dependence of closed times on calcium is controversial in the literature. Our results support the data of Chu et al. (1993) but are at odds with those of Ashley and Williams (1990) and Sitsapesan and Williams (1994), as we did not observe changes in any of the three closed lifetimes over the calcium concentration range we used. Channel transitions related to binding of activating calcium are, in accordance to Györke and Fill (1993), faster than our time resolution.

Our data show that increased P_o at high Ca^{2+} (Ashley and Williams, 1990; Chu et al., 1993; Sitsapesan and Williams, 1994) is due in part to distinct calcium dependence of the relative proportions of the individual closed time components (Table 1). The contribution of the fast components increases whereas that of the slow component decreases with Ca^{2+} concentration. At very low Ca^{2+} concentrations, it is reasonable to ascribe long closures to sojourns of the channel at the resting (calcium-free) state. At high calcium concentrations, however, the persistence of very long closures (τ_{c3} ~150 ms contributing 20% at 50 μM Ca^{2+}, see Table 1), observed unequivocally in every report, cannot be explained by transitions to the resting state (Zahradníková and Palade, 1993) or by missed events (see Results section). Therefore we conclude that the long closures of the channel under these conditions originate from entering an inactivated "mode."

Modes of CRC gating

By applying standard methods of modal analysis developed originally for voltage-activated calcium channels (Hess et al., 1984; Nowycky et al., 1985) together with our "nest" analysis, it was possible to demonstrate the existence of at least three modes of activity of the CRC. Several lines of evidence indicate that the three types of observed behavior can be defined as modes. First, channel open probability has a bimodal distribution that shows two well separated peaks in frequency histograms. Second, higher P_o of the channel is closely correlated with both longer openings and higher frequency of openings. Third, the two active modes differ primarily in the relative probability of observing particular components of overall open, closed, and burst distributions. Fourth, transitions between the modes proceed on a slow time scale of ~1 s, which gives rise to nonrandom distribution of channel gating patterns when analyzed on a segment-to-segment basis.

The channels were found to be very homogenous in mean state lifetimes, in open probabilities within modes, and in all other quantitative parameters characterizing modal behavior. On the other hand, individual channels varied widely in relative occurrence of the three modes of activity, resulting in a large scatter of the open probabilities. Large scatter of P_o was also reported by Sitsapesan and Williams (1994) for the cardiac CRC and by Shomer et al. (1993) for the skeletal muscle CRC. Therefore, to interpret single-channel behavior of the CRC correctly, e.g., for studying modulation of CRC activity by external molecules, long stretches of data must be collected and analyzed.

Kinetics of intermodal transitions

The distributions of mode duration were reasonably well fitted by single exponentials, given the low number of transitions. As mode lifetimes are comparable to the segment length, many short-lived transitions between modes must have remained undetected. Short H-mode sojourns undetected within mode L may be the source of long opening events as well as of bursts detected in L-mode segments. Whether L-mode sojourns within segments marked as H-mode could give rise to the measured ~50% proportion of short openings, ~16% of single open events, and ~30% of short bursts in mode H, or whether both open states are available in this mode, remains to be determined.

The large differences in single-channel properties of the three channel modes resulting in the ability of the channel to switch between three widely different levels of open probability (including zero) could have important physiological implications. The channel inhibitor procaine exerts its effect by binding to the long-lived closed state of the channel (Zahradníková and Palade, 1993), which could be interpreted as stabilization of mode I (see Hess et al., 1984).

Modal gating and adaptation

Steady-state characteristics of the CRC determined in this work parallel, in several respects, features of CRC adaptation described by Györke and Fill (1993) and Györke et al. (1994) under almost the same experimental conditions. First, lifetime of H-mode is very close to the time constant of CRC adaptation (0.86 vs. 1.3 s). Second, open probability during H-mode (~0.2, see Table 3) is four times higher than the overall open probability of ~0.05 (Table 1), the differ-

ence of which can be compared with the amplitude of adaptation. Third, high open probability bursts can be observed at the onset of calcium pulses (Györke and Fill, 1993) resembling H-mode bursts. These findings, together with other properties of modes, suggest the hypothesis that CRC adaptation is a transition of the channel from mode H to the equilibrium mixture of all modes.

Our preliminary results of modeling and simulations (Zahradníková and Zahradník, 1995) show that preferential rapid access to mode H upon channel activation by Ca^{2+} results in transient channel responses that have single-channel properties compatible with the experimentally measured data. These results will be the subject of a separate communication. In this respect it is important to note that skeletal muscle CRC, which displays the same time course of activity during adaptation as does the cardiac CRC (Györke et al., 1994), also shows correlations of gating suggestive of modal behavior (Vélez et al., 1993). The use of ATP and Mg^{2+} in the experimental solutions speeds up inactivation of the CRC (Valdivia et al., 1995) to such an extent that recognition of modes could be difficult with our software. It was important for this study to keep experimental conditions close to the conditions under which adaptation was described (Györke and Fill, 1993).

A question that remains is whether modal behavior of the channel arises from some kind of external regulation or whether it reflects transitions within a simple, externally nonregulated gating structure. Our experiments were done with CRCs of crude SR preparation in which interactions between the measured channel and other proteins of SR membrane (including silent channels) are possible. These interactions, apparently of physiological importance, are not likely to influence the lifetime parameters of the channel, as Sitsapesan and Williams (1994) have found no differences in channel open and closed times between native and purified CRC. We have observed very stable values of these parameters, when analyzed for different segment types, and little channel-to-channel variation as well. These findings almost exclude the possibility that external modulation, if present, influences transitions on the time scale of milliseconds. However, an external factor might affect rates of transitions between modes. Other active interactions may be slower still or permanent (e.g., a covalent modification such as phosphorylation, ribosylation, or change of redox state) and thus might contribute to channel-to-channel variation in long-term distribution of modes (see Fig. 2 *D*, *crossed circles*, where heterogeneity of L-mode occurrence is obvious). This variation in mode occupancy suggests that at least a modulatory role of some external factor, acting on a slow time scale and having no effect on rapid kinetics of the channel, is possible. Heterogeneity in response to modulators of CRCs, homogenous with respect to their rapid gating kinetics, was observed for skeletal (Ma, 1995) as well as for cardiac CRCs (Zahradníková et al. 1995). In terms of our hypothesis that modal behavior and adaptation share the same molecular basis, the effects of such interaction, which was used to explain the absence of adaptation in purified CRCs (Vélez et al., 1995), could be experimentally tested employing the purified preparation.

In conclusion, the results presented here provide evidence that in steady state the cardiac CRC undergoes slow changes of activity on the time scale of seconds attributable to the presence of three gating modes: mode I when the channel is not available for opening, mode L with a vast majority of single open events coming from the shorter open state, and mode H with a high occurrence of bursts composed of openings from the longer open state. Modal gating might provide the basis for understanding the mechanism of action of certain inhibitors (Zahradníková and Palade, 1993), of CRC adaptation (Györke and Fill, 1993), and of the the molecular mechanisms of its physiological function in general.

The authors wish to thank S. Györke for his valuable comments, P. Doris for reading the manuscript, and E. Ríos and I. Stavrovský for providing access to their manuscript before publication.

REFERENCES

Ashley, R. H., and A. J. Williams. 1990. Divalent cation activation and inhibition of single calcium release channels from sheep cardiac sarcoplasmic reticulum. *J. Gen. Physiol.* 95:981–1005.

Bezprozvanny, I., J. Watras, and B. E. Ehrlich. 1991. Bell-shaped calcium-response curves of $Ins(1,4,5)P_3$- and calcium-gated channels from endoplasmic reticulum of cerebellum. *Nature*. 351:751–754.

Blatz, A. L., and K. L. Magleby. 1986. Quantitative description of three modes of activity of fast chloride channels from rat skeletal muscle. *J. Physiol.* 378:141–174.

Cannell, M. B., J. R. Berlin, and W. J. Lederer. 1987. Effect of membrane potential changes on the calcium transient in single rat cardiac muscle cells. *Science*. 238:1419–1423.

Chu, A., M. Fill, E. Stefani, and M. L. Entmann. 1993. Cytoplasmic Ca^{2+} does not inhibit the cardiac muscle sarcoplasmic reticulum ryanodine receptor Ca^{2+} channel, although Ca^{2+}-induced Ca^{2+} inactivation of Ca^{2+} release is observed in native vesicles. *J. Membrane Biol.* 135: 49–59.

Cleeman, L., and M. Morad. 1991. Role of Ca^{2+} channel in cardiac excitation-contraction coupling in the rat: evidence from Ca^{2+} transients and contraction. *J. Physiol.* 432:283–312.

Colquhoun, D., and A. G. Hawkes. 1983. The principles of the stochastic interpretation of ion-channel mechanisms. *In* Single Channel Recording. B. Sakmann and E. Neher, editors. Plenum Press, New York. 135–175.

Colquhoun, D., and F. J. Sigworth. 1983. Fitting and statistical analysis of single-channel records. *In* Single Channel Recording. B. Sakmann and E. Neher, editors. Plenum Press, New York. 191–263.

Fabiato, A. 1985. Time and calcium dependence of activation and inactivation of calcium-induced calcium release of calcium from the sarcoplasmic reticulum of a skinned canine cardiac Purkinje cell. *J. Gen. Physiol.* 85:247–289.

Fabiato, A. 1988. Computer programs for calculating total from specified free or free from specified total ionic concentration in aqueous solutions containing multiple metals and ligands. *Methods Enzymol.* 157: 378–417.

Fisher, R. A. 1958. Statistical Methods for Research Workers. Oliver and Boyd, Edinburgh.

Fox, A. P., P. Hess, J. B. Lansman, B. Nilius, M. C. Nowycky, and R. W. Tsien. 1986. Shifts between modes of calcium channel gating as a basis for pharmacological modulation of calcium influx in cardiac, neuronal, and smooth-muscle-derived cells. *In* New Insights into Cell and Membrane Transport Processes. G. Poste and S. T. Crooke, editors. Plenum Press, New York. 99–123.

Györke, S., and M. Fill. 1993. Ryanodine receptor adaptation: control mechanism of Ca^{2+}-induced Ca^{2+} release in heart. *Science*. 260: 807–809.

Györke, S., P. Vélez, B. Suárez-Isla, and M. Fill. 1994. Activation of single cardiac and skeletal ryanodine receptor channels by flash photolysis of caged Ca^{2+}. *Biophys. J.* 66:1879–1886.

Hamilton, S. L., R. Mejia Alvarez, M. Fill, M. J. Hawkes, K. L. Brush, W. P. Schilling, and E. Stefani. 1989. [^{3}H]PN200–110 and [^{3}H]ryanodine binding and reconstitution of ion channel activity with skeletal muscle membranes. *Anal. Biochem.* 183:31–41.

Harigaya, S., and A. Schwartz. 1969. Rate of calcium binding and uptake in normal animal and failing human cardiac muscle. *Circ. Res.* 25: 781–794.

Hess, P., J. B. Lansman, and R. W. Tsien. 1984. Different modes of Ca channel gating favoured by dihydropyridine Ca agonists and antagonists. *Nature*. 311:538–544.

Imredy, J. P., and D. T. Yue. 1994. Mechanism of Ca^{2+}-sensitive inactivation of L-type Ca^{2+} channels. *Neuron*. 12:1301–1318.

Ma, J. 1995. Desensitization of the skeletal muscle ryanodine receptor: evidence for heterogeneity of calcium release channels. *Biophys. J.* 68:893–899.

Magleby, K. L., and B. S. Pallotta. 1983. Burst kinetics of single calcium-activated potassium channels in cultured rat muscle. *J. Physiol.* 344: 605–623.

Näbauer, M., G. Callewaert, L. Cleeman, and M. Morad. 1989. Regulation of calcium release is gated by calcium current, not gating charge, in cardiac myocytes. *Science*. 244:800–803.

Nowycky, M. C., A. P. Fox, and R. W. Tsien. 1985. Long-opening mode of gating of neuronal calcium channels and its promotion by the dihydropyridine calcium agonist Bay K 8644. *Proc. Natl. Acad. Sci. USA*. 82:2178–2182.

Patlak, J. B., K. A. F. Gration, and P. N. R. Usherwood. 1979. Single glutamate-activated channels in locust muscle. *Nature*. 278:643–645.

Patlak, J. B., and M. Ortiz. 1985. Slow currents through single sodium channels of the adult rat heart. *J. Gen. Physiol.* 86:89–104.

Rousseau, E., and G. Meissner. 1989. Single cardiac sarcoplasmic reticulum Ca^{2+}-release channel: activation by caffeine. *Am. J. Physiol.* 256: H328–H333.

Shomer, N. H., C. F. Louis, M. Fill, A. Litterer, and J. R. Mickelson. 1993. Reconstitution of abnormalities in the malignant hyperthermia-susceptible pig ryanodine receptor. *Am. J. Physiol.* 264:C125–C135.

Sipido, K., and W. G. Wier. 1991. Flux of calcium across the sarcoplasmic reticulum of guinea-pig cardiac cells during excitation-contraction coupling. *J. Physiol.* 435:605–630.

Sitsapesan, R., and A. J. Williams. 1994. Gating of the native and purified cardiac SR Ca^{2+}-release channel with monovalent cations as permeant species. *Biophys. J.* 67:1484–1494.

Smith, J. S., T. Imagawa, J. Ma, M. Fill, K. P. Campbell, and R. Coronado. 1988. Purified ryanodine receptor from rabbit skeletal muscle is the calcium-release channel of sarcoplasmic reticulum. *J. Gen. Physiol.* 92:1–26.

Valdivia H. H., J. H. Kaplan, G. C. R. Ellies-Davies, and W. J. Lederer. 1995. Rapid adaptation of cardiac ryanodine receptors: modulation by Mg^{2+} and phosphorylation. *Science*. 267:1997–2000.

Vélez, P., R. Armisén, J. Sierralta, A. Ocampo, J. Vergara, and B. A. Suárez-Isla. 1993. Temporal correlations in Ca^{2+} release reveal modal gating. *Biophys. J.* 64:380*a*. (Abstr.)

Vélez, P., X. Li, R. Tsushima, M. Cortez-Gutierrez, A. Wasserstrom, and M. Fill. 1995. Adaptation of single cardiac ryanodine receptor channels may involve a closely associated regulatory protein. *Biophys. J.* 68:375*a*. (Abstr.)

Zahradníková, A., J. Bak, and L. G. Mészáros. 1995. Heterogeneity of the cardiac calcium release channel as assessed by its response to ADP-ribose. *Biochem. Biophys. Res. Commun.* 210:457–463.

Zahradníková, A., and P. Palade. 1993. Procaine effects on single sarcoplasmic reticulum Ca^{2+} release channels. *Biophys. J.* 64:991–1003.

Zahradníková, A., and I. Zahradník. 1993. Modelling time-resolved activation and inactivation of the single cardiac calcium release channel activated by calcium ions. 11th International Biophysics Congress, Budapest, Hungary. C2.37, p.122. (Abstr.)

Zahradníková, A., and I. Zahradník. 1995. The role of modal behavior in the inactivation of cardiac Ca^{2+}-release channels. *Biophys. J.* 68:374*a*. (Abstr.)